+Supplementary data for

A Spirocyclic BODIPY Photosensitizer with pH-Triggered Triplet-State Activation for Tumor-Selective Photodynamic Therapy

Luying Guo,[a] Xing Guo,[a*] Yiran Liu,[a] Heng Li,[a] Huiquan Zuo,[a*] Shaozhen Wang,[b] Lijuan Jiao,[a] and Erhong Hao[a*]

[a]*The Key Laboratory of Functional Molecular Solids of Ministry of Education, Anhui Province Key Laboratory of Biomedical Materials and Chemical Measurement, School of Chemistry and Materials Science, Anhui Normal University, Wuhu 241002, China.*

[b]*Institute of Synthesis and Application of Medical Materials, Department of Pharmacy, Wannan Medical College, Wuhu 241002, China.*

E-mail: *guoxing@ahnu.edu.cn; huiquan.zuo@ahnu.edu.cn; haoehong@ahnu.edu.cn*

Table of contents

1. General Information

Reagents and solvents were used as received from commercial suppliers unless noted otherwise. Cremophor EL (CrEL, co-solvent surfactant), 1,3-Diphenylisobenzofuran (DPBF), 2,2,6,6-tetramethyl-4-piperidone (TEMP), 5,5-dimethyl-1-pyrroline-N-oxide (DMPO), 2', 7'-dichlorofluorescin diacetate (DCFH-DA), dihydroethidium (DHE), 1,7-diphenyl-2,6-dibromo-3,5-di(4-methoxyphenyl)-azaBODIPY (**aza-BDP**), LysoTracker Green DND-26 (DND-26) and nigericin were purchased from commercial supplier and used directly. All reactions were performed in oven-dried or flame-dried glassware unless stated otherwise and were monitored by TLC using 0.25 mm silica gel plates with UV indicator (60F-254). $^{1}H/^{13}C$ NMR spectra were recorded on 400 MHz NMR spectrometer at room temperature. Chemical shifts (δ) are given in ppm relative to $CDCl_3$ (7.26 ppm for ^{1}H and 77.0 ppm for ^{13}C NMR) or Acetone-d_6 (2.05 ppm for ^{1}H NMR) to internal tetramethylsilane (TMS, δ = 0.0 ppm). High-resolution mass spectra (HRMS) were obtained using ESI in positive mode. Cells morphologies were observed using a confocal laser scanning microscopy (CLSM, Leica Microsystems SP8 MP).

Absorption and emission measurements

UV-visible absorption and fluorescence emission spectra were recorded on commercial spectrophotometers (Hitachi U-4100 and Edinburgh FLS-1000 spectrometers, 300-700 nm scan range) at room temperature (10 mm quartz cuvette). Absolute fluorescence quantum efficiencies of BODIPY derivatives were measured by absolute PL quantum yield spectrometer (Hamamatsu, C11347) in integrating sphere, using Eq. S1 given below:[1]

$$\Phi_{FL} = \frac{N_{em}}{N_{abs}} = \frac{\alpha \int \frac{\lambda}{hc} I_{em}(\lambda) d\lambda}{\alpha \int \frac{\lambda}{hc} [I_{ex}(\lambda) - I'_{ex}(\lambda)] d\lambda} \quad \text{Eq. S1}$$

where N_{em} and N_{abs} are the numbers of emitted and absorbed photons, respectively, α is the calibration factor for the measurement setup, λ is the wavelength, h is the Planck's constant, c is the speed of light, $I_{em}(\lambda)$ is the emission intensity at λ, and $I_{ex}(\lambda)$ and $I'_{ex}(\lambda)$ are the intensities of the excitation laser beam with λ in the absence and presence of the sample, respectively. The measured Φ_{FL} values are independent of sharp and thickness of sample and power of excitation laser.

Theoretical calculation

The ground state geometry was optimized by using DFT method at M062X/def2TZVP level for **2**, **BDP** and **BDP-I**. The same method was adopted for vibrational analysis to verify that the optimized structures correspond to local minima on the energy surface (no imaginary frequencies). TD-DFT calculations were performed at M062X/def2TZVP theoretical level. The molecule calculations in water were using the Self-

Consistent Reaction Field (SCRF) method and Solvation Model based on solute electron Density (SMD). All of the calculations were carried out by the methods implemented in Gaussian 09 package.[2]

Calculation of pK_a values

The pK_a[3] value of **BDP-I** was estimated from the changes in fluorescence intensity observed at various pH values using the relationship, $\log[(I_{max}-I)/(I-I_{min})] = pH - pK_a$, where I_{max}, I_{min}, and I are the maximum, minimum, and observed fluorescence intensities at a given pH, respectively. The pK_a value (y-intercept) for **BDP-I** ($pK_a = 6.869 \pm 0.0363$) was derived from a plot of pH *vs* $\log[(I_{max}-I)/(I-I_{min})]$. This plot is shown in Figure S6. Other information is available in the figure captions.

Singlet oxygen detection

A comparative study of the relative singlet oxygen generating efficiency of these dyes was performed in air-saturated solvents under light at 660 nm laser irradiation (2.79 mW/cm^2) condition using 1,3-diphenylisobenzofuran (DPBF, 4×10^{-5} M) as a trap molecule. A commercial photosensitizer against 1,7-diphenyl-2,6-dibromo-3,5-di(4-methoxyphenyl)-azaBODIPY (**aza-BDP**) ($\Phi_\Delta = 0.74$ in toluene) was used as reference.[4] The absorbance of BODIPY dyes and the reference **aza-BDP** at 660 nm was kept around 0.1. The decrease of the absorbance band of 1,3-diphenylisobenzofuran at 415 nm was monitored. Singlet oxygen quantum yield (Φ_Δ) determinations were carried out using the chemical trapping method, and the Φ_Δ value was obtained by the relative method using **aza-BDP** as the reference as shown in following equation:

$$\Phi_{\triangle sam} = \Phi_{\Delta ref}\,[(m_{sam}/m_{ref})\,(L_{ref}/L_{sam})]$$

Where $\Phi_{\Delta ref}$ and $\Phi_{\Delta sam}$ are the singlet oxygen quantum yields for the standard **aza-BDP** and photosensitizer (**BDP-I**). m_{sam} and m_{ref} are the slope of the difference (ΔO.D.) in the change in the absorption maximum wavelength of 1,3-diphenylisobenzofuran (415 nm), which are plotted against the photoirradiation time, L_{ref} and L_{sam} are the light harvesting efficiency, which is given by $L = 1\text{-}10^{-A}$ ("A" is the absorbance at the laser irradiation wavelength 660 nm).

Preparation of BDP-I micelles

BDP-I (15.0 μL, 1.0 mM in DMSO) and Cremophor EL (10.0 μL, 0.33%, *v/v*, 60.0 mg mL^{-1} in DMSO) were mixed uniformly, then diluted with 3.0 mL PBS or cell culture medium to afford **BDP-I** micelles.

Cells culture

HeLa and 4T1 cells were cultured in culture media (RPMI-1640, supplemented with 10% FBS and 1% penicillin/streptomycin solution) at 37 °C in an atmosphere of 5% CO_2 and 95% humidified atmosphere.

HUVEC and RAW 264.7 cells were cultured in culture media (Dulbecco's Modified Eagle Medium, High Glucose, supplemented with 10% FBS and 1% penicillin/streptomycin solution) at 37 °C in an atmosphere of 5% CO_2 and 95% humidified atmosphere.

Dark toxicity determined by the CCK-8 method

The HeLa cells (5000) per well were seeded on 96-well plates and incubated in RPMI-1640 complete medium for 12 h at 37 °C. Then, a gradient concentration of **BDP-I** micelles from 0.0 to 5.0 μM in a fresh medium were added into the 96-well plate, and the cells with **BDP-I** micelles were incubated at 37 °C for 24 h. After that, the working solutions were then removed. A total of 100.0 μL of Cell Counting Kit-8 (diluted 10-fold, CCK-8, BIOMIKY) was added into each well, and the cells were further incubated at 37 °C for 30 min in a 5% CO_2 humidified atmosphere. The plate was shaken for 5 min, and the absorbance was measured at 450 nm using a microplate reader (Multiskan Sky). The viability of HeLa cells was calculated by the following equation:[5]

$$\text{Cell viability (\%)} = (OD_{dye} - OD_{blank\ control}) / (OD_{control} - OD_{blank\ control}) \times 100\% \quad \text{Eq. S2}$$

OD_{dye}, $OD_{control}$, $OD_{blank\ control}$ stand for the absorbance of cells containing dye, cell control (without dye) and blank control (containing neither cells nor dyes), respectively.

Photodynamic cytotoxicity determined by the CCK-8 method

The HeLa cells (5000) per well were seeded on 96-well plates and incubated in RPMI-1640 complete medium for 12 h at 37 °C. Then, a gradient concentration of **BDP-I** micelles from 0.0 to 5.0 μM in a fresh medium were added into the 96-well plate, and the cells with **BDP-I** micelles were incubated at 37 °C for 12 h, The experimental group of the cells were illuminated with a LED lamp (filter: 610 nm, 19.2 mW/cm^2) for 1 h at room temperature. Then these cells were followed by a 11 h incubation solely in the dark (total 24 h) in the incubator. The control groups of the cells were incubated in the dark, for the duration of 24 h under identical experimental conditions except illumination. After that, the working solutions were then removed. A total of 100.0 μL of Cell Counting Kit-8 (diluted 10-fold, CCK-8, BIOMIKY) was added into each well, and the cells were further incubated at 37 °C for 30 min in a 5% CO_2 humidified atmosphere. The plate was shaken for 5 min, and the absorbance was measured at 450 nm using a microplate reader (Multiskan Sky).

Cell incubation and colocalization imaging

HeLa cells were stained with **BDP-I** micelles (5.0 μM, 10 h) and LysoTracker Green DND-26 (DND-26, 0.05 μM, 0.5 h, lysosomes commercial dye) at 37 ºC in an atmosphere of 5% CO_2. Finally, the morphologies of the HeLa cells were observed using a confocal laser scanning microscopy (CLSM, Leica Microsystems SP8 MP, For DND-26, λ_{ex}: 488 nm, λ_{em} :500~540 nm; For **BDP-I** micelles: λ_{ex}: 638 nm, λ_{em} :650~750 nm).

Intracellular pH response

HeLa cells were treated with **BDP-I** micelles (5.0 μM) and incubated in the incubator for 10 h. After that, the cells were treated with PBS (containing 10.0 μM nigericin) at different pH (5.0, 6.0, 7.0, 8.0) values for 15 min. [6] Finally, the morphologies of the HeLa cells were observed using a CLSM (Leica Microsystems SP8 MP, λ_{ex}: 638 nm; λ_{em}: 650-750 nm).

Live-dead cell staining

Live-dead cell staining analysis was also performed to evaluate cell viability. Briefly, a total of 30000 HeLa cells were seeded into a glass bottom dish and were cultured in culture media (RPMI-1640, supplemented with 10% FBS) at 37 °C in an atmosphere of 5% CO_2 and 95% humidified atmosphere for 12 h. Cells in control-1 wells were incubated in the incubator for 10 h. Cells in control-2 wells were treated with **BDP-I** micelles (5.0 μM) and were kept in the dark in the same condition for 10 h. Cells in control-3 were incubated for 10 h and then the cells were irradiated with a 660 nm laser (8.29 mW/cm^2) for 10 min. Cells in control-4 were incubated with **BDP-I** micelles (5.0 μM) for 10 h and then the cells were irradiated with a 660 nm laser (8.29 mW/cm^2) for 10 min. The cells were then replaced with AO-PI[7] mixture in the dark at room temperature. Finally, the morphologies of the HeLa cells were observed using a CLSM (Leica Microsystems SP8 MP, For AO: λ_{ex}: 488 nm, λ_{em} :498~540 nm; For PI, λ_{ex}: 552 nm, λ_{em}: 566~640 nm).

Cellular ROS detection

HeLa cells were seeded at a density of 30000 cells in glass-bottom dishes and incubated at 37 °C with 5% CO_2 for 12 h. Cells in control-1 wells were incubated in the incubator for 10 h, then incubated with DCFH (10.0 μM, 1 h). Cells in control-2 wells were treated with **BDP-I** micelles (5.0 μM) and were kept in the dark in the same condition for 10 h, then incubated with DCFH (10.0 μM, 1 h). Cells in control-3 were incubated for 10 h, then incubated with DCFH (10.0 μM, 1 h) and then the cells were irradiated with a 660 nm laser (8.29 mW/cm^2) for 10 min without the **BDP-I** micelles. Cells in control-4 were incubated with **BDP-I** (5.0 μM) for 10 h, then incubated with DCFH (10.0 μM, 1 h) and then the cells were irradiated with a 660 nm laser

(8.29 mW/cm^2) for 10 min. Finally, the morphologies of the HeLa cells were observed using a CLSM (Leica Microsystems SP8 MP, Green channel: λ_{ex}: 488 nm, λ_{em}: 500-620 nm).

HeLa cells were seeded at a density of 30000 cells in glass-bottom dishes and incubated at 37 °C with 5% CO_2 for 12 h. Cells in control-1 wells were incubated in the incubator for 10 h, then incubated with DHE (10.0 μM, 1 h). Cells in control-2 wells were treated with **BDP-I** micelles (5.0 μM) and were kept in the dark in the same condition for 10 h, then incubated with DHE (10.0 μM, 1 h). Cells in control-3 were incubated for 10 h, then incubated with DHE (10.0 μM, 1 h) and then the cells were irradiated with a 660 nm laser (8.29 mW/cm^2) for 10 min without the **BDP-I** micelles. Cells in control-4 were incubated with **BDP-I** micelles (5.0 μM) for 10 h, then incubated with DHE (10.0 μM, 1 h) and then the cells were irradiated with a 660 nm laser (8.29 mW/cm^2) for 10 min. Finally, the morphologies of the HeLa cells were observed using a CLSM (Leica Microsystems SP8 MP, Red channel: λ_{ex}: 552 nm, λ_{em}: 570-690 nm).

Statistical analysis

Quantitative data are presented as the mean ± standard deviation (SD) herein. One-way ANOVA with a post-hoc Tukey's test was used for statistical analysis. The p-value less than 0.05 were considered as statistically significant. All statistical analyses were performed using OriginPro 2021 software (plug-in: paired comparison plot; p values: *$p < 0.05$, **$p < 0.01$, ***$p < 0.001$).

2. Synthesis and Characterization

Compound **1** was synthesized according to the literature.[8]

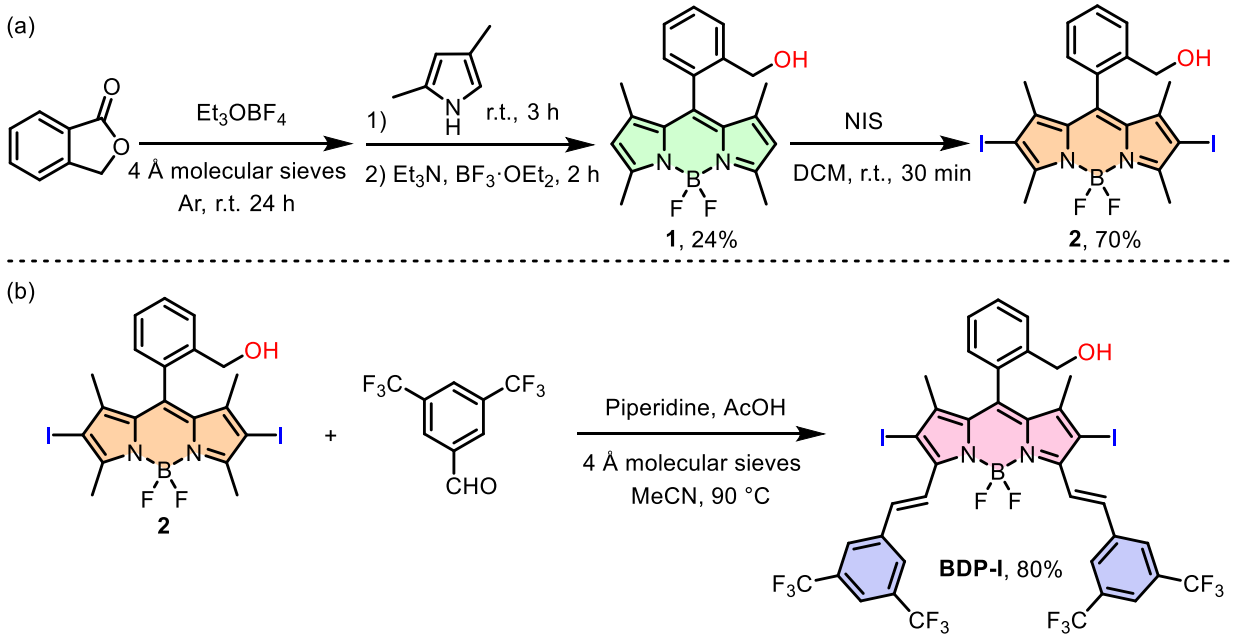

Scheme S1. Synthesis of **BDP-I**.

Synthesis of 1[8]: To a 100 mL dry round-bottom flask, add phthalide (1.45 g, 10.8 mmol) and preactivated 4 Å molecular sieves (200 mg/mmol, 2.16 g). The freeze-pump-thaw cycle was carried out three times. Then, add Et_3OBF_4 (1.0 mol/L in dichloromethane, 10.8 mL) to the round-bottom flask under argon. The resulting solution was stirred for 24 h. After cooling to 0 °C, 2,4-dimethylpyrrole (3.13 mL, 29.5 mmol) was added and the resulting mixture stirred under argon at room temperature for an additional 3 h. After cooling to 0 °C again, Et_3N (9.0 mL, 64.8 mmol) and $BF_3{\cdot}OEt_2$ (12.0 mL, 97.2 mmol) were added dropwise and stirred at room temperature for another 2 h. The residue was extracted with CH_2Cl_2, washed with H_2O, dried over Na_2SO_4, and concentrated under reduced pressure. The crude product was further purified using column chromatography (eluent: ethyl acetate and petroleum ether = 1/10, *v*/*v*) on silica gel to afford the BODIPY **1** in 24% (920 mg) isolated yield as orange powder. ^{1}H NMR (400 MHz, $CDCl_3$) δ 7.65 (d, J = 7.7 Hz, 1H), 7.51 (td, J = 7.6, 1.2 Hz, 1H), 7.42 (t, J = 7.0 Hz, 1H), 7.20 (dd, J = 7.5, 0.9 Hz, 1H), 5.98 (s, 2H), 4.59 (s, 2H), 2.55 (s, 6H), 1.36 (s, 6H).

Synthesis of 2: A mixture of **1** (100 mg, 0.28 mmol) and NIS (140 mg, 0.62 mmol) in DCM (5 mL) was stirred at room temperature for 30 min. And the reaction was quenching by $Na_2S_2O_3$ aqueous solution. The residue was extracted with CH_2Cl_2, washed with H_2O, dried over Na_2SO_4, and concentrated under reduced pressure. The crude product was further purified using column chromatography (eluent: ethyl acetate and petroleum ether = 1/4 – 1/6, *v*/*v*) on silica gel to afford the BODIPY **2** in 70% (120 mg) isolated yield as red

powder. ^{1}H NMR (400 MHz, $CDCl_3$) δ 7.69 (d, J = 7.7 Hz, 1H), 7.57 (t, J = 7.6 Hz, 1H), 7.45 (t, J = 7.5 Hz, 1H), 7.16 (d, J = 7.5 Hz, 1H), 4.57 (s, 2H), 2.65 (s, 6H), 1.38 (s, 6H). ^{13}C NMR (100 MHz, $CDCl_3$) δ 157.1, 145.1, 139.4, 138.0, 132.6, 130.8, 130.2, 128.7, 128.4, 127.9, 85.8, 62.3, 16.5, 16.1 ppm. HRMS (ESI) m/z calcd. For $C_{20}H_{20}BF_2I_2N_2O^+$, $[M+H]^+$ 606.9721, found 606.9719.

Synthesis of BDP-I: A mixture of **2** (30 mg, 0.05 mmol), 3,5-bis(trifluoromethyl)benzaldehyde (41 μL, 0.25 mmol), preactivated 4 Å molecular sieves (100 mg), piperidine (30 μL) and AcOH (30 μL) in MeCN (5 mL) was stirred at 90 ℃ for 30 min. After reaction, the solvent was removed and recovered by distillation. The residue was extracted with CH_2Cl_2, washed with NH_4Cl/H_2O and $NaHCO_3/H_2O$, dried over Na_2SO_4, and concentrated under reduced pressure. The crude product was further purified using column chromatography (eluent: ethyl acetate and petroleum ether = 1/3 – 1/5, *v*/*v*) on silica gel to afford the **BDP-I** in 80% (42 mg) isolated yield as dark blue powder.^{1}H NMR (400 MHz, $CDCl_3$) δ 8.19 (d, J = 16.8 Hz, 2H), 8.02 (s, 4H), 7.85 (s, 2H), 7.82 – 7.71 (m, 3H), 7.63 (t, J = 7.4 Hz, 1H), 7.52 (t, J = 7.4 Hz, 1H), 7.24 (d, J = 7.7 Hz, 1H), 4.64 (s, 2H), 1.49 (s, 6H). ^{13}C NMR (100 MHz, $CDCl_3$) δ 149.9, 149.6, 146.9, 139.6, 138.5, 138.1, 136.2, 133.2, 132.6, 132.4 (q, $^{2}J_{C2\text{-}F}$ = 33.0 Hz), 130.6, 129.0, 128.7, 128.0, 124.5 (q, $^{1}J_{C1\text{-}F}$ = 261.0 Hz), 122.4 (q, $^{3}J_{C3\text{-}F}$ = 4.0 Hz), 121.8, 84.1, 62.4, 17.1 ppm. HRMS (ESI) m/z calcd. For $C_{38}H_{23}BF_{14}I_2N_2O^+$, $[M]^+$:1053.9764, found 1053.9764.

3. Photophysical Properties

Table S1. Photophysical properties of **2** and **BDP-I** in different solvents at room temperature.

Dyes	Solvent	λ_{abs}^{max} (nm)	λ_{em}^{max} (nm)	Stokes shift (cm^{-1})[a]	ε (M^{-1} cm^{-1})[b]	Φ_{FL}[c]
2	Hexane	534	550	550	70300	0.042
	Toluene	538	555	570	68900	0.020
	DCM	536	554	610	66400	0.015
	THF	534	552	610	67100	0.030
	MeOH	532	551	650	64100	0.015
BDP-I	Hexane	631	653	530	80700	0.150
	Toluene	638	665	640	102900	0.120
	DCM	634	660	620	103800	0.101
	THF	632	658	630	105600	0.100
	MeOH	628	652	590	97800	0.100

[a]The Stokes shift values are rounded to the nearest 10 cm^{-1}. [b]Corresponding to the strongest absorption maximum. [c]Fluorescence quantum yields were measured by absolute fluorescence quantum yield spectrometer (Hamamatsu) using integrating sphere[1]. The standard errors are less than 5%.

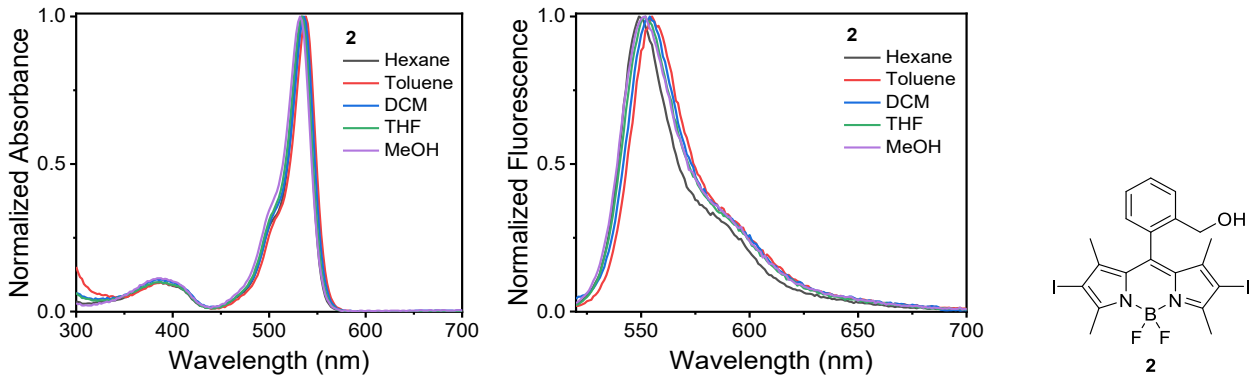

Figure S1. Normalized absorption (left) and emission (right) spectra of compound **2** recorded in different solvents. λ_{ex}: 520 nm.

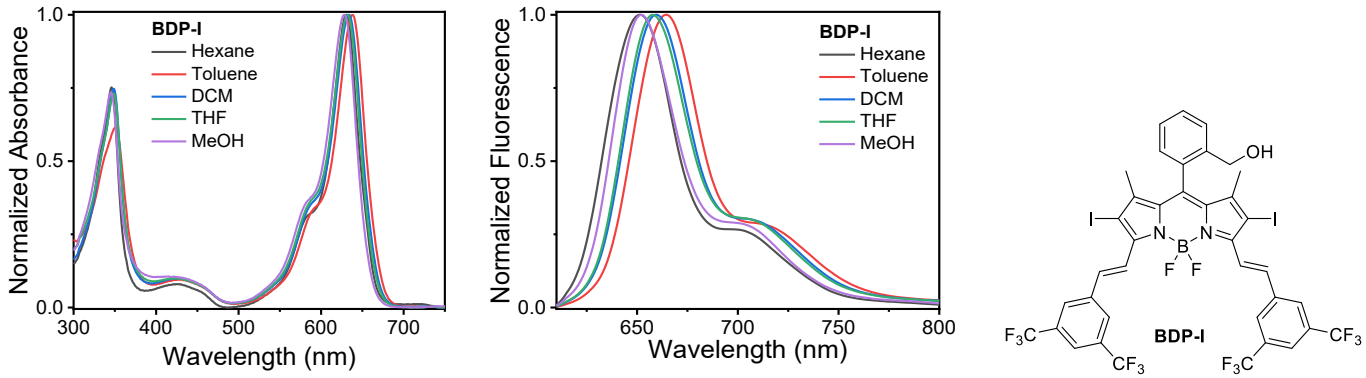

Figure S2. Normalized absorption (left) and emission (right) spectra of compound **BDP-I** recorded in different solvents. λ_{ex}: 600 nm.

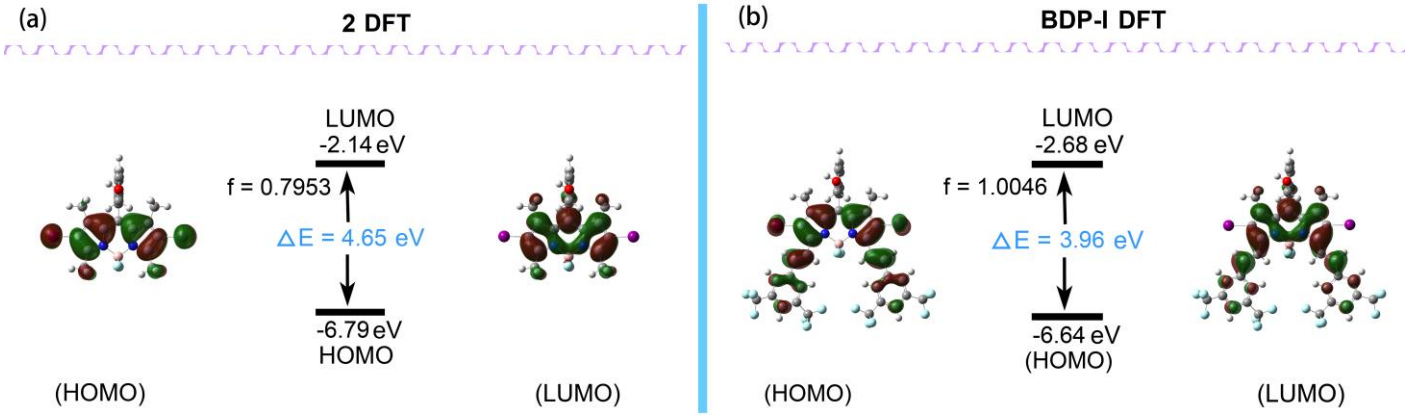

Figure S3. Molecular orbital amplitude plots of HOMO and LUMO energy levels of **2** (a) and **BDP-I** (b) at M062X/def2TZVP level (SMD, in water).

Table S2. HOMO and LUMO energies of **2** and **BDP-I** calculated at the M062X/def2TZVP level using the Gaussian 09 program package.[2]

	Electronic transition	**TD//M062X/def2TZVP**			
		Energy/ eV [a]	***f* [b]**	**Composition [c]**	**CI [d]**
2	$S_0 \rightarrow S_1$	2.7199 eV 457.18 nm	0.7953	HOMO → LUMO	0.7009
	$S_0 \rightarrow S_2$	3.6974 eV 335.32 nm	0.0800	HOMO -2 → LUMO	0.1586
				HOMO -1 → LUMO	0.6729
	$S_0 \rightarrow S_3$	3.8762 eV 319.86 nm	0.0789	HOMO -2 → LUMO	0.6589
				HOMO -1 → LUMO	0.1550
BDP-I	$S_0 \rightarrow S_1$	2.2378 eV 554.04 nm	1.0046	HOMO → LUMO	0.6974
	$S_0 \rightarrow S_2$	3.3814 eV 366.67 nm	0.0744	HOMO -2 → LUMO	0.6848
	$S_0 \rightarrow S_3$	3.5719 eV 347.11 nm	0.2424	HOMO -3 → LUMO	0.3673
				HOMO -1 → LUMO	0.5792

[a] Only the selected low-lying excited states are presented. [b] Oscillator strength. [c] Only the main configurations are presented. [d] The CI (configuration interaction) coefficients are in absolute values.

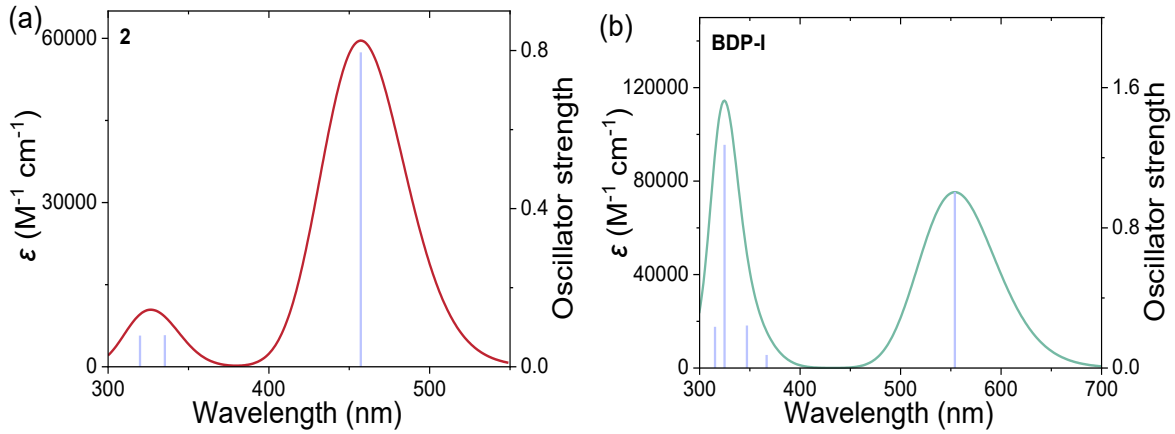

Figure S4. Calculated absorption bands for **2** (a) and **BDP-I** (b) at M062X/def2TZVP level (SMD, in water).

Table S3. Selected molecular LUMO (lowest unoccupied molecular orbital, Multiwfn[9]) distribution in **BDP-I** skeleton by DFT calculations (M062X/TZVP).

Atoms	LUMO percentage
C7 (*meso*-position)	18.09%
C6 (*α*-position)	8.50%
C11 (*α*-position)	8.40%

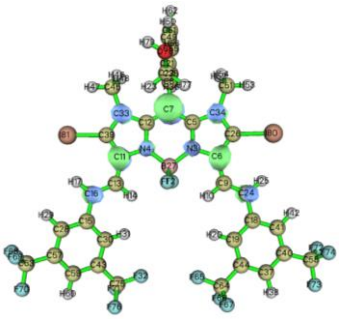

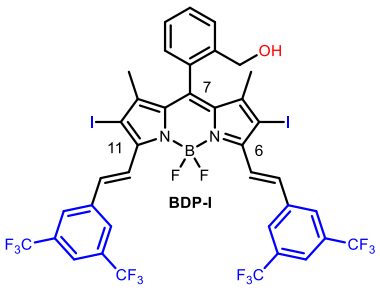

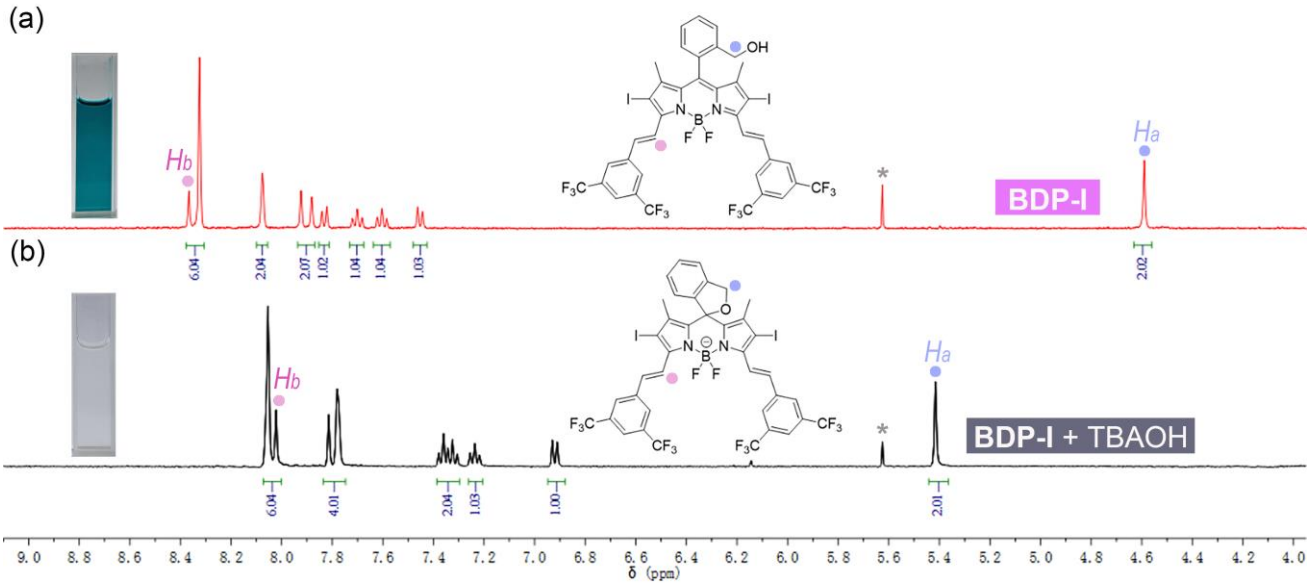

Figure S5. pH titration process of **BDP-I:** ^{1}H NMR spectra of **BDP-I** in acetone-d_6 before (a) and after (b) the addition of 20.0 μL TBAOH (Tetrabutylammonium Hydroxide, 1.0 M). *Represented DCM solvent peak.

For **BDP-I**: ^{1}H NMR (400 MHz, Acetone-d_6) δ 8.35 (d, J = 16.8 Hz, 6H), 8.08 (s, 2H), 7.90 (d, J = 17.0 Hz, 2H), 7.83 (d, J = 7.8 Hz, 1H), 7.70 (t, J = 7.9 Hz, 1H), 7.60 (t, J = 7.3 Hz, 1H), 7.45 (d, J = 7.4 Hz, 1H), 4.59 (s, 2H), 1.55 (s, 6H).

For **BDP-I + TBAOH**: ^{1}H NMR (400 MHz, Acetone-d_6) δ 8.04 (d, J = 12.8 Hz, 6H), 7.80 (d, J = 13.6 Hz, 4H), 7.39 – 7.30 (m, 2H), 7.24 (t, J = 7.3 Hz, 1H), 6.92 (d, J = 7.6 Hz, 1H), 5.42 (s, 2H), 1.61 (s, 6H).

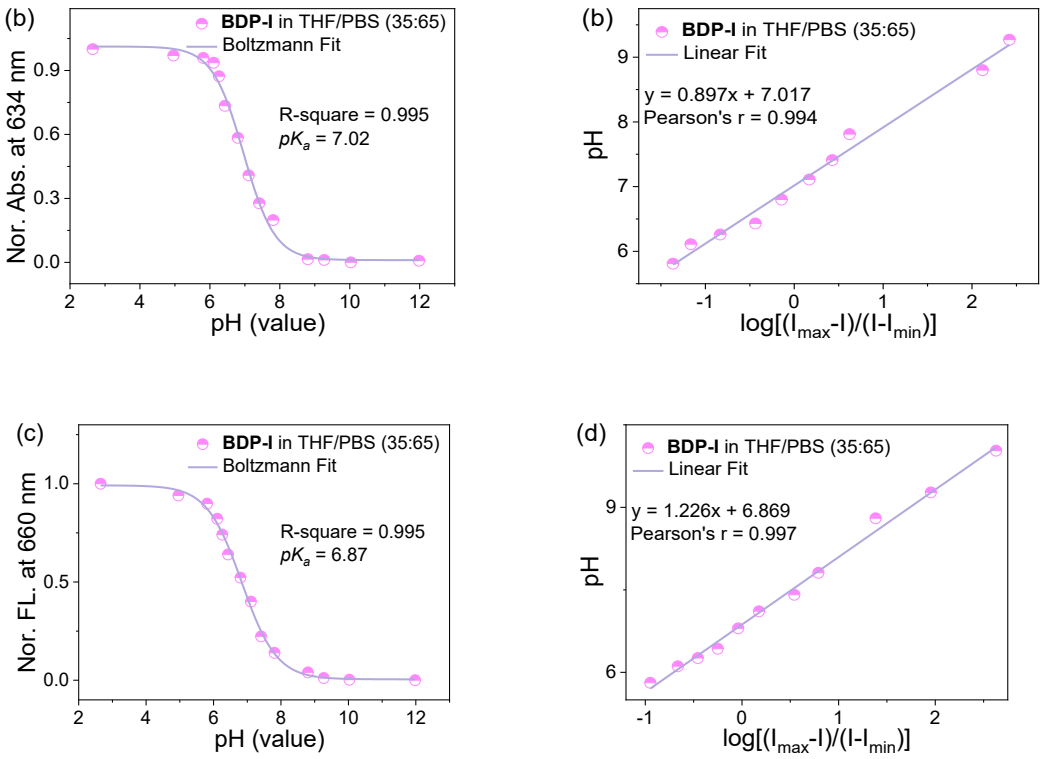

Figure S6. (a) Plot of the absorption at 634 nm *versus* different pH values. (b) Log[(I $_{max}$ - I)/(I - I $_{min}$)] = pH - pK_a, the pK_a value of **BDP-I** was calculated to be 7.02. (absorption spectra, 634 nm). (c) Plot of the normalized fluorophore intensity at 660 nm *versus* different pH values. (d) Log[(I_{max} - I)/(I - I_{min})] = pH - pK_a, the pK_a[3] value of **BDP-I** was calculated to be 6.87 (emission spectra, 660 nm).

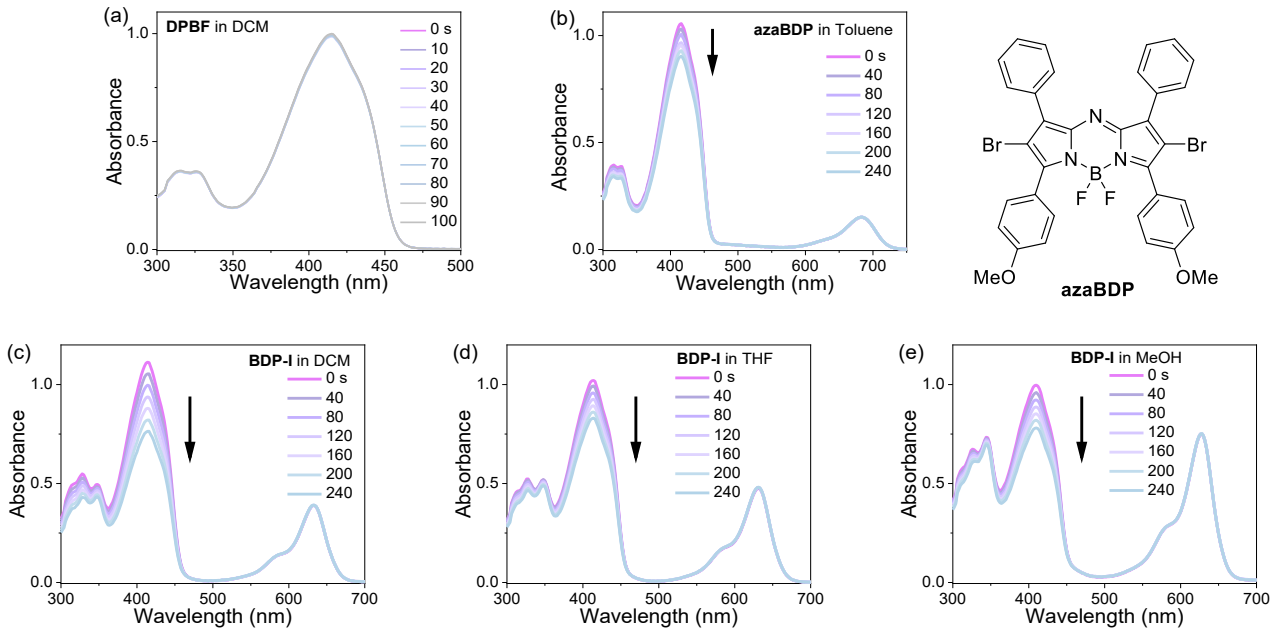

Figure S7. (a) The absorbance of 1,3-diphenylisobenzofuran (DPBF) in DCM under irradiation of a 660 nm laser (2.79 mW/cm^2). (b) The absorbance of DPBF in the presence of **aza-BDP** in toluene under irradiation of a 660 nm laser (2.79 mW/cm^2). (c-e) The absorbance of DPBF in the presence of **BDP-I** in different solvents under irradiation of a 660 nm laser (2.79 mW/cm^2).

Table S4. Comparison of 1,3-diphenylisobenzofuran degradation rate in the presence of **aza-BDP** and **BDP-I** respectively at 414 nm under irradiation (660 nm) as a function of irradiation time.

Dyes	Solvent	λ_{abs}[a]/nm (ε[b])	λ_{em}^{max}/nm (Φ_{FL}[c])	ROS efficiency[d] **BDP-I/aza-BDP**
BDP-I	Toluene	638 (102900)	665 (0.12)	1.14
	DCM	634 (103800)	660 (0.10)	1.75
	THF	632 (105600)	658 (0.10)	1.02
	MeOH	628 (97800)	652 (0.10)	1.14

[a]Main absorption maxima. [b]Corresponding to the strongest absorption maximum. ($M^{-1}cm^{-1}$). [c] Fluorescence quantum yields were measured by absolute fluorescence quantum yield spectrometer (Hamamatsu) using integrating sphere[1]. [d]Relative efficiency of reactive oxygen species with **aza-BDP** (Φ_Δ = 0.74 in Toluene) as the reference.[4]

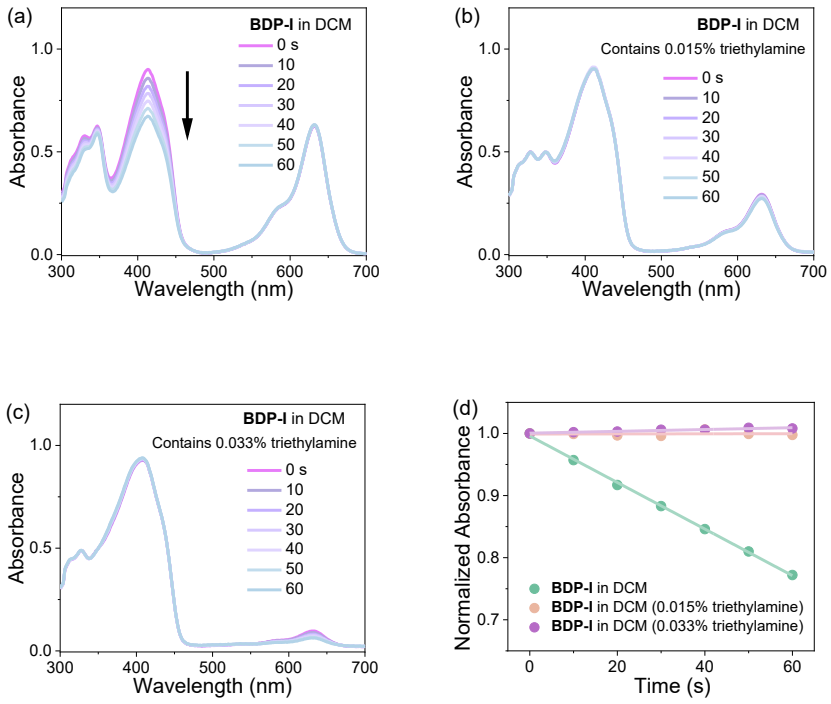

Figure S8. (a) The absorbance of 1,3-diphenylisobenzofuran (DPBF) in the presence of **BDP-I** in DCM under irradiation of a 660 nm laser (3.42 mW/cm^2). (b) The absorbance of DPBF in the presence of **BDP-I** in DCM (containing 0.015% triethylamine) under irradiation of a 660 nm laser (3.42 mW/cm^2). (c) The absorbance of DPBF in the presence of **BDP-I** in DCM (containing 0.033% triethylamine) under irradiation of a 660 nm laser (3.42 mW/cm^2).

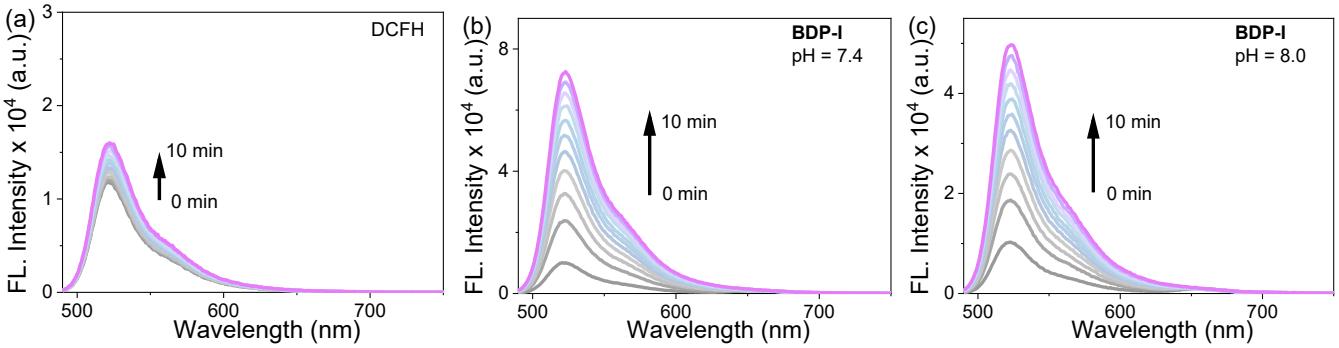

Figure S9. (a) Emission spectrum of DCFH (40.0 μM) in PBS (pH = 7.4) under irradiation of a 660 nm laser (2.79 mW/cm^2). (b, c) Emission spectrum of DCFH (40.0 μM) in the presence of **BDP-I** (containing 0.33% Cremophor EL, *v/v*) in PBS *versus* different pH under irradiation of a 660 nm laser (2.79 mW/cm^2). λ_{ex}: 470 nm.

4. Cellular Studies

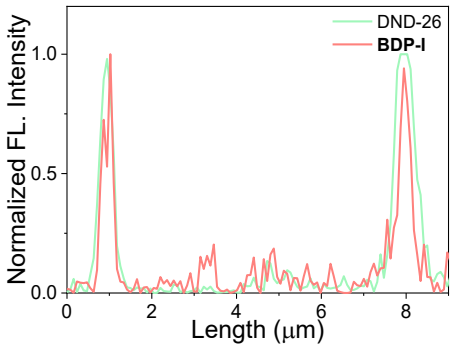

Figure S10. Intensity profiles within the regions of interests of LysoTracker Green DND-26 (DND-26) and **BDP-I** micelles across HeLa cells, Pearson's correlation Rr = 0.88 ± 0.02.

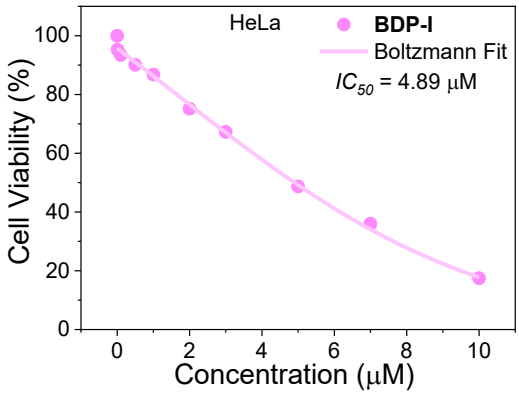

Figure S11. Curve fitting between the HeLa cell viability and the concentration of **BDP-I** micelles. IC_{50} = 4.89 μM. Error bars represent the standard deviation of per group (n = 6).

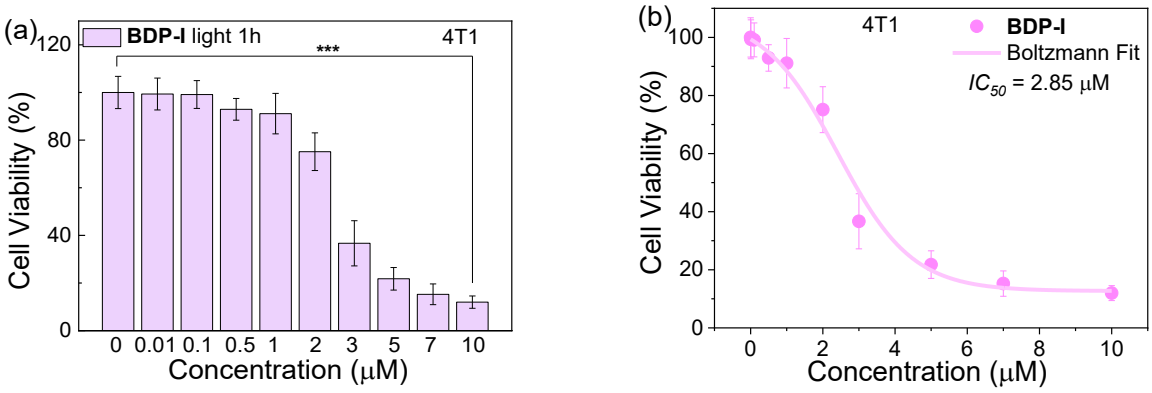

Figure S12. (a) The 4T1 cells with **BDP-I** micelles were incubated at 37 °C for 12 h, then the cells were illuminated with a LED lamp (filter: 610 nm, 19.2 mW/cm^2) for 1 h. (b) Curve fitting between the cell viability and the concentration of **BDP-I** micelles. IC_{50} = 2.85 μM. Error bars represent the standard deviation of per group (n = 6; Error bars are SD; one-way ANOVA followed by Tukey's test; **P < 0.01, ***P < 0.001; significant).

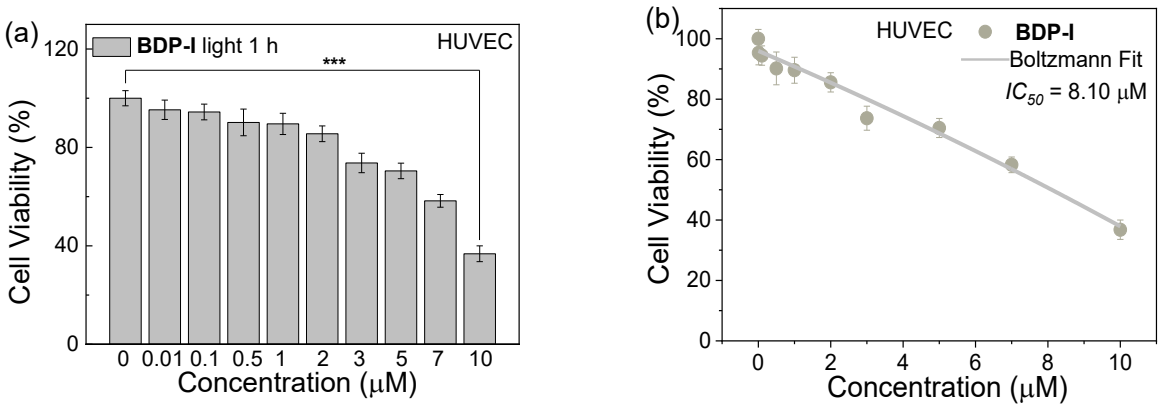

Figure S13. (a) The HUVEC cells with **BDP-I** micelles were incubated at 37 °C for 12 h, then the cells were illuminated with a LED lamp (filter: 610 nm, 19.2 mW/cm^2) for 1 h. (b) Curve fitting between the cell viability and the concentration of **BDP-I** micelles. IC_{50} = 8.10 μM. Error bars represent the standard deviation of per group (n = 6; Error bars are SD; one-way ANOVA followed by Tukey's test; **P < 0.01, ***P < 0.001; significant).

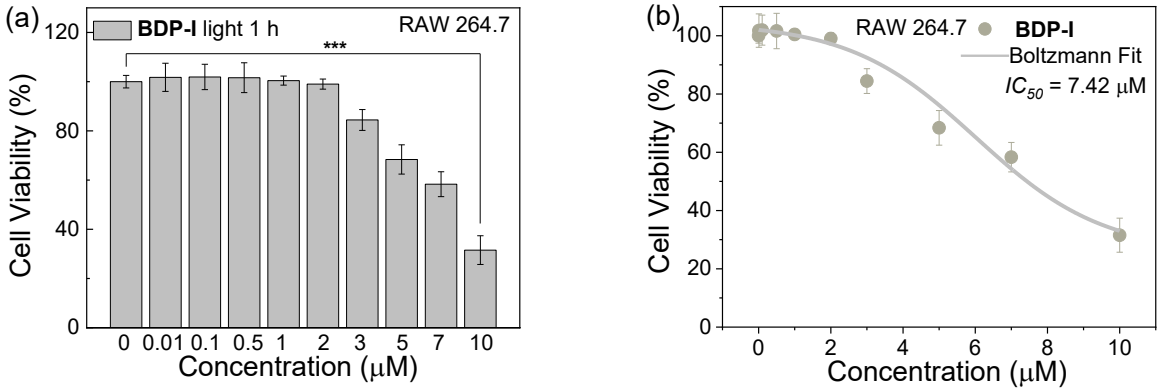

Figure S14. (a) The RAW 264.7 cells with **BDP-I** micelles were incubated at 37 °C for 12 h, then the cells were illuminated with a LED lamp (filter: 610 nm, 19.2 mW/cm^2) for 1 h. (b) Curve fitting between the cell viability and the concentration of **BDP-I** micelles. IC_{50} = 7.42 μM. Error bars represent the standard deviation of per group (n = 6; Error bars are SD; one-way ANOVA followed by Tukey's test; **P < 0.01, ***P < 0.001; significant).

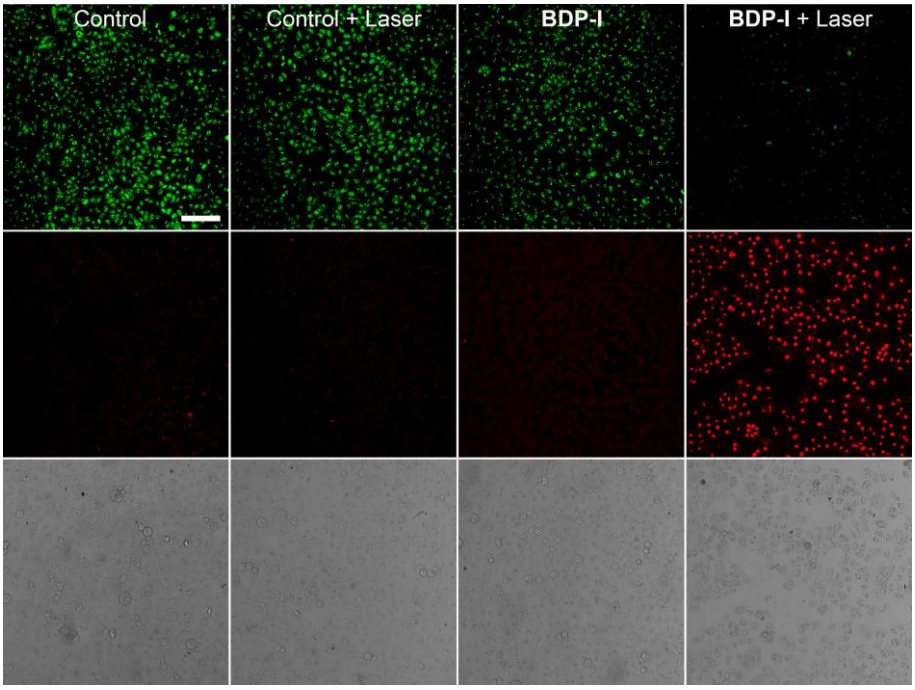

Figure S15. Fluorescence images of AO (green) and PI (red) co-staining HeLa cells incubated with 0, or 5.0 μM of **BDP-I** micelles (5.0 μM) without and with laser irradiation (660 nm, 8.29 mW/cm^2). For AO: λ_{ex}: 488 nm, λ_{em} :498~540 nm; For PI, λ_{ex}: 552 nm, λ_{em}: 566~640 nm. Scale bar: 100 μm.

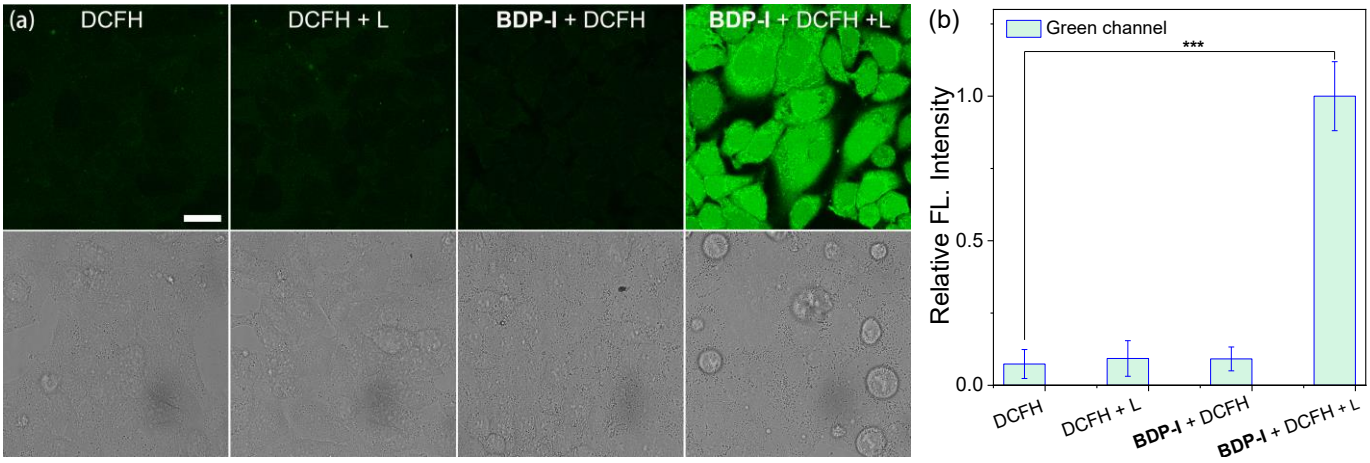

Figure S16. (a) Confocal fluorescence images of ROS generation in HeLa cells after incubation with **BDP-I** micelles (5.0 μM) using DCFH-DA (10.0 μM) as a ROS indicator under laser exposure. (660 nm, 8.29 mW/cm^2). (b) Relative fluorescence intensity quantitation was analyzed by the images. λ_{ex}: 488 nm, λ_{em}: 500~620 nm. scale bar: 25 μm. (n = 10; Error bars are SD; one-way ANOVA followed by Tukey's test; **P < 0.01, ***P < 0.001; significant).

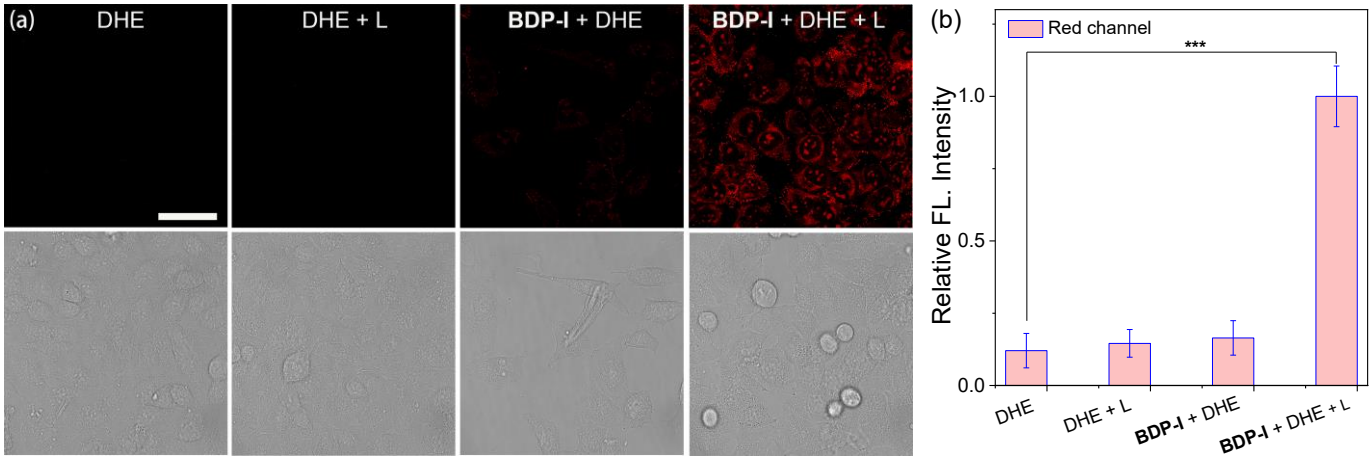

Figure S17. Confocal fluorescence images of ROS generation in HeLa cells after incubation with **BDP-I** micelles (5.0 μM) using DHE (10.0 μM)·as a $O_2^{\bullet-}$ indicator under laser exposure (660 nm, 8.29 mW/cm^2). (b) Relative fluorescence intensity quantitation was analyzed by the images. λ_{ex}: 552 nm, λ_{em}: 570~690 nm. scale bar: 50 μm. (n = 10; Error bars are SD; one-way ANOVA followed by Tukey's test; **P < 0.01, ***P < 0.001; significant).

5. DFT Optimized Molecular Coordinates

DFT optimized S_0 state Geometry of **2**.

0 1

F	-0.03323500	-3.02498400	1.19215000
F	0.01068700	-3.19264800	-1.07452200
N	1.23803900	-1.38018600	-0.04881900
N	-1.25387200	-1.37876600	-0.07996800
C	1.20810400	-0.00077600	-0.18986300
C	2.52014900	-1.79698300	-0.02099300
C	-0.00389900	0.68415700	-0.28517000
C	0.00013600	2.15543200	-0.50026900
C	-2.53575700	-1.78346500	0.02682300
C	-1.21859100	0.00087000	-0.21030300
C	0.04971800	3.03352500	0.58540100
C	0.07990500	2.47320200	1.98893300
H	-0.77974100	1.80791500	2.12836600
C	3.33702000	-0.64532500	-0.11319800
B	-0.00970100	-2.29981200	-0.00119400
C	-2.55369700	0.49447500	-0.19152700
C	2.54742300	0.48273700	-0.22146000
C	-0.03611500	2.63639200	-1.80378900
H	-0.07542900	1.93452000	-2.62862000
C	-3.34726000	-0.62682000	-0.04466400
C	-3.03284500	1.90274800	-0.27747500
H	-2.65782200	2.49055100	0.56281200
H	-4.12076300	1.92714500	-0.25299300
H	-2.69424500	2.38483400	-1.19455800
C	0.06706000	4.40037200	0.33486300
H	0.10745000	5.09408900	1.16492600
C	3.03650600	1.88825400	-0.29892400
H	2.61081900	2.41416400	-1.15322200
H	4.12131200	1.89960500	-0.38832400
H	2.76193500	2.44261400	0.60110000
C	-0.01883500	4.00468400	-2.04113100
H	-0.04642500	4.37807900	-3.05681200
C	0.03310500	4.88450400	-0.96871700
H	0.04739200	5.95307400	-1.14370300
H	0.98213700	1.86991400	2.11759100
O	0.11359200	3.46170600	3.00192300
H	-0.72917800	3.93262600	3.00025800
I	5.43412700	-0.62058800	-0.00581000
I	-5.44685700	-0.60140100	-0.01233700
C	-2.86763300	-3.19943600	0.15857600
H	-2.32783800	-3.76197600	-0.57427500
H	-2.59976100	-3.53898600	1.13727400
H	-3.91847300	-3.33486500	0.00926800
C	2.84672900	-3.21586400	0.09124800
H	3.59147000	-3.46891100	-0.63416900
H	3.22126000	-3.41909600	1.07273800
H	1.96675200	-3.79923500	-0.08258400

SCF done: -1778.316181 Hartree

No imaginary Frequency.

DFT optimized S_0 state Geometry of **BDP**.

0 1

F	-1.31619600	0.01553100	0.98584900
F	-1.37906100	-0.01140600	-1.28503100
N	0.38754300	-1.24644100	-0.17884200
N	0.39326700	1.24119400	-0.20815500
C	1.77660700	-1.21927100	-0.24566100
C	-0.01557100	-2.53292800	-0.12809900
C	2.46547400	-0.00917200	-0.31056900
C	3.94713900	-0.01590400	-0.45127300
C	-1.41271500	-2.90111000	-0.07099500
H	-2.12989500	-2.08959900	-0.06798000
C	-0.00253500	2.53065500	-0.17021600
C	1.78162500	1.20551400	-0.27776300
C	-1.39737700	2.90726100	-0.11009500
H	-2.11983600	2.10047700	-0.12297900
C	-3.18876000	4.64821100	0.02257600
C	-1.80227500	4.18439300	-0.03946600
H	-1.05583600	4.97356400	-0.02026900
C	-3.21537100	-4.63256800	0.02886300
C	-4.31072600	-3.75825700	0.00727400
H	-4.15429600	-2.68844300	-0.05458600
C	4.77150700	-0.02469300	0.67710800
C	4.14217500	-0.02424200	2.05146400
H	3.43940400	0.81286700	2.12558200
C	-1.82598700	-4.17671100	-0.02556400
H	-1.08469700	-4.97089900	-0.02603400
B	-0.52737200	-0.00009000	-0.17227800
C	-3.42479600	6.02349100	0.12800400
H	-2.57950900	6.70157500	0.15858700
C	-4.28980500	3.78179100	-0.01784400
H	-4.14040200	2.71251600	-0.10230600
C	2.25863300	2.55011800	-0.26950200
C	2.24582100	-2.56710900	-0.22190400
C	4.49625500	-0.02031200	-1.72831800
H	3.83747600	-0.01336900	-2.58899800
C	-5.83388900	-5.62269300	0.14033700
H	-6.84716600	-6.00187300	0.18330500
C	-4.75719900	-6.50020000	0.16093500
C	-3.46032300	-6.00821600	0.10516800
H	-2.61947700	-6.69232300	0.12095100
C	-5.58006800	4.28144700	0.04821800
C	-5.60420200	-4.25080200	0.06306700
C	3.67053400	3.03681800	-0.28485800
H	4.21580800	2.69082500	0.59605300
H	3.67741800	4.12618400	-0.28612300
H	4.21342800	2.68336900	-1.16232200
C	6.14964000	-0.04073800	0.49779700

H	6.79977600	-0.05030500	1.36340700
C	3.65428100	-3.06381800	-0.23386500
H	4.20140800	-2.71452600	-1.11041200
H	3.65294200	-4.15320600	-0.23511100
H	4.20055800	-2.72254400	0.64811300
C	5.87512700	-0.03353700	-1.89618200
H	6.29923100	-0.03587100	-2.89223700
C	-4.71845300	6.52265200	0.19392800
C	-5.80085400	5.65285600	0.15456800
H	-6.81165200	6.03761900	0.20557900
C	6.70008900	-0.04359000	-0.77982000
H	7.77628600	-0.05454400	-0.89997700
H	3.56687500	-0.94414600	2.18352600
O	5.07827700	0.01809600	3.11327600
H	5.51698100	0.87806300	3.10072400
H	-4.92629900	-7.56809500	0.22008500
H	-6.44054600	-3.56311500	0.04529700
H	-6.42081600	3.59968900	0.01596000
H	-4.88058100	7.59013500	0.27581600
C	1.12410300	-3.36738600	-0.14951700
H	1.11667500	-4.44564300	-0.11311200
C	1.14164100	3.35807400	-0.20470800
H	1.14056500	4.43675000	-0.18226800

SCF done: -2370.889444 Hartree
No imaginary Frequency.

DFT optimized S_0 state Geometry of **BDP-I**.

0 1

F	-0.11621100	0.07823600	0.98286700
F	0.13160800	0.03485400	-1.27645700
N	1.23908700	1.79857800	-0.04916500
N	-1.23995200	1.78142500	-0.30345700
C	1.20393100	3.18333900	-0.11816500
C	2.51892500	1.39132700	0.07109800
C	-0.00355400	3.86257000	-0.28488000
C	0.00052500	5.34337400	-0.41955900
C	2.84957600	-0.01598900	0.13534200
H	2.01819300	-0.66709400	0.37447100
C	-2.52089100	1.36108800	-0.33386300
C	-1.21111400	3.16635800	-0.35594800
C	-2.84183100	-0.04967600	-0.30872800
H	-2.01669700	-0.70542600	-0.55776400
C	-4.33777700	-2.00454500	0.05494800
C	-4.03156800	-0.57170500	0.01897900
H	-4.85341500	0.07120000	0.30691200
C	4.36912400	-1.97414500	-0.06832800
C	3.39086400	-2.96760700	0.07500900
H	2.34567500	-2.70266500	0.16179700
C	-0.05819700	6.16129900	0.71169400
C	-0.14587500	5.52549800	2.08021400

H	-1.00581500	4.84662300	2.10615200
C	4.05825900	-0.54214300	-0.10436300
H	4.89526100	0.09404700	-0.36176500
C	3.32574300	2.55290700	0.11437100
B	0.00410800	0.86760400	-0.16296000
C	-5.61959100	-2.39536000	0.43715200
H	-6.35300600	-1.63907300	0.69432300
C	-3.40591000	-2.99885500	-0.26935900
H	-2.40011900	-2.73519100	-0.56922100
F	-1.50590900	-4.95549800	-0.51964500
C	-2.54888000	3.64732600	-0.43049700
C	2.53435100	3.67873500	-0.00360200
C	0.07428600	5.89442700	-1.69341200
H	0.11771300	5.23830600	-2.55488600
C	5.08615800	-4.69290200	-0.03041800
H	5.35410700	-5.74213500	-0.01655800
C	-3.33774700	2.51327100	-0.41569400
C	6.04644600	-3.71045500	-0.17414700
C	5.69977000	-2.36466200	-0.19784000
H	6.46809600	-1.60852600	-0.31594900
C	-3.76320900	-4.33135300	-0.20090500
C	3.75584300	-4.29856700	0.09160700
C	-3.03670800	5.05424700	-0.48342500
H	-2.74568500	5.59835900	0.41739900
H	-4.12270700	5.06842100	-0.55529600
H	-2.62405300	5.58838900	-1.33929100
C	-0.03635200	7.53987500	0.53736400
H	-0.07906800	8.18757600	1.40370000
C	3.01010300	5.09031700	0.03855700
H	2.65541200	5.65857400	-0.82103200
H	4.09832100	5.11535300	0.04750300
H	2.64928200	5.59249400	0.93876500
C	0.09487500	7.27372500	-1.85454700
H	0.15302000	7.70174300	-2.84712600
C	-5.96100000	-3.74077900	0.49254500
C	7.49821100	-4.07079900	-0.30816300
C	-5.04461800	-4.72538100	0.17416000
H	-5.31061400	-5.77350100	0.21914700
C	0.03966000	8.09411700	-0.73617300
H	0.05560400	9.17072300	-0.85163000
C	-7.35795400	-4.10076300	0.91036700
C	2.71730800	-5.37560200	0.23040800
F	1.47838100	-4.88880400	0.34659600
F	2.71466800	-6.20287900	-0.82862400
F	2.93854400	-6.14696500	1.30814800
F	-8.27672800	-3.59448600	0.07081200
F	-7.65441600	-3.61697800	2.12794500
F	-7.55821200	-5.42153500	0.95600200
F	-2.96520900	-5.84283900	-1.82900800
F	8.03120400	-3.58131800	-1.43973300
F	7.70358400	-5.39143900	-0.31932300
F	8.23127700	-3.56941800	0.70005000
C	-2.76851700	-5.39331600	-0.57676900

F	-2.84963500	-6.46452700	0.22597400
H	0.74906500	4.92344800	2.25670400
O	-0.21538700	6.45750200	3.14368000
H	-1.06070100	6.92094000	3.09172100
I	5.40445000	2.58880600	0.41049500
I	-5.43203000	2.51980800	-0.57040100

SCF done: -3664.955924 Hartree
No imaginary Frequency.

6. Scanned NMR and HRMS Spectra

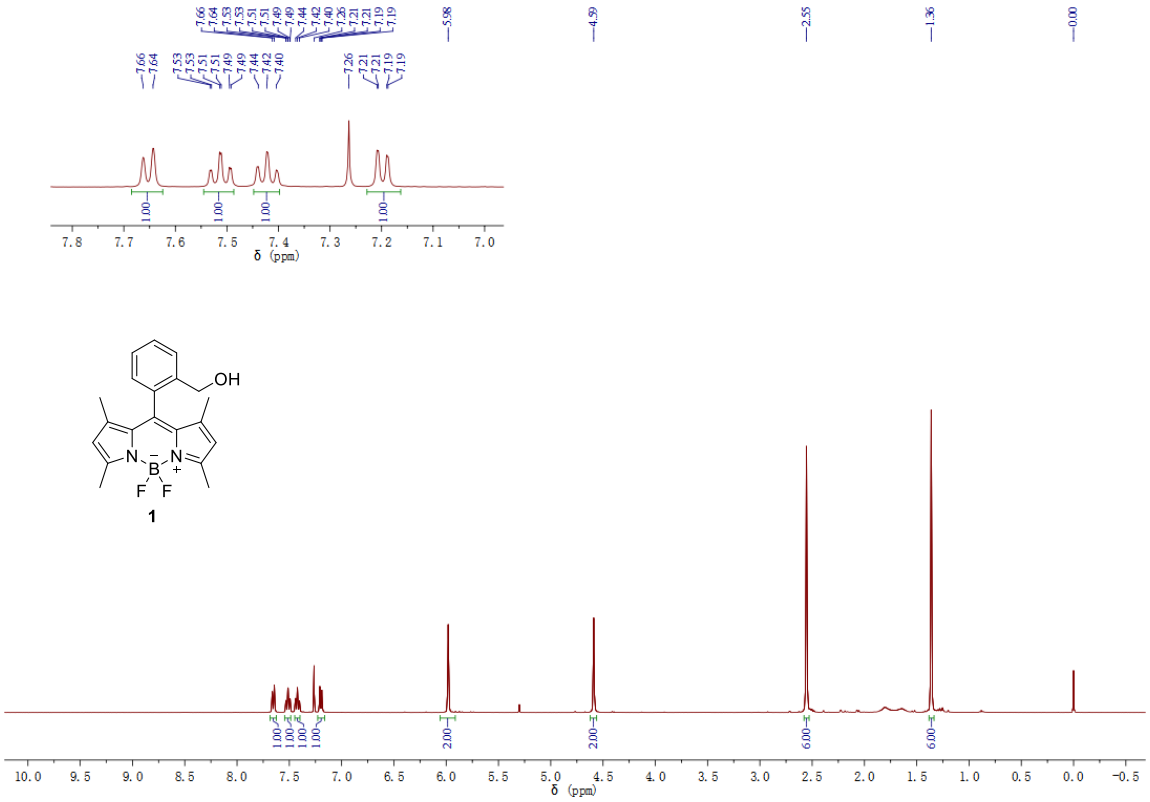

^{1}H NMR of **1** in $CDCl_3$ (400 MHz).

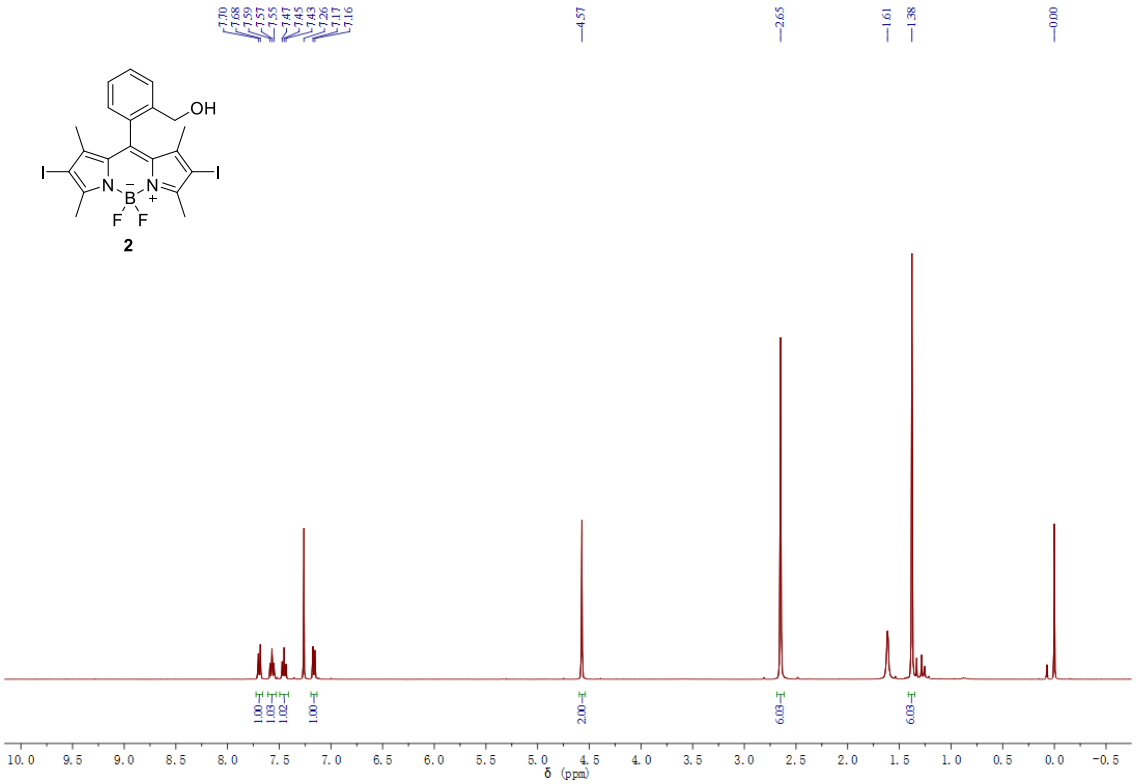

^{1}H NMR of **2** in $CDCl_3$ (400 MHz).

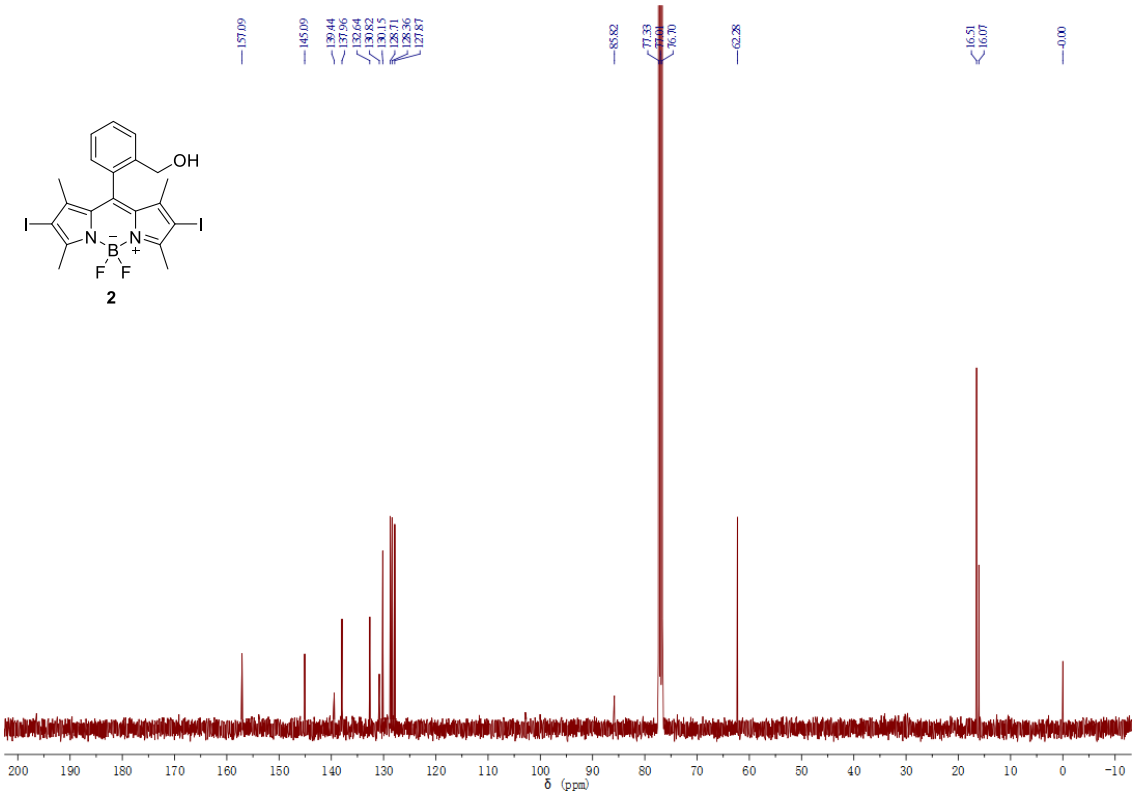

^{13}C NMR of **2** in $CDCl_3$ (100 MHz).

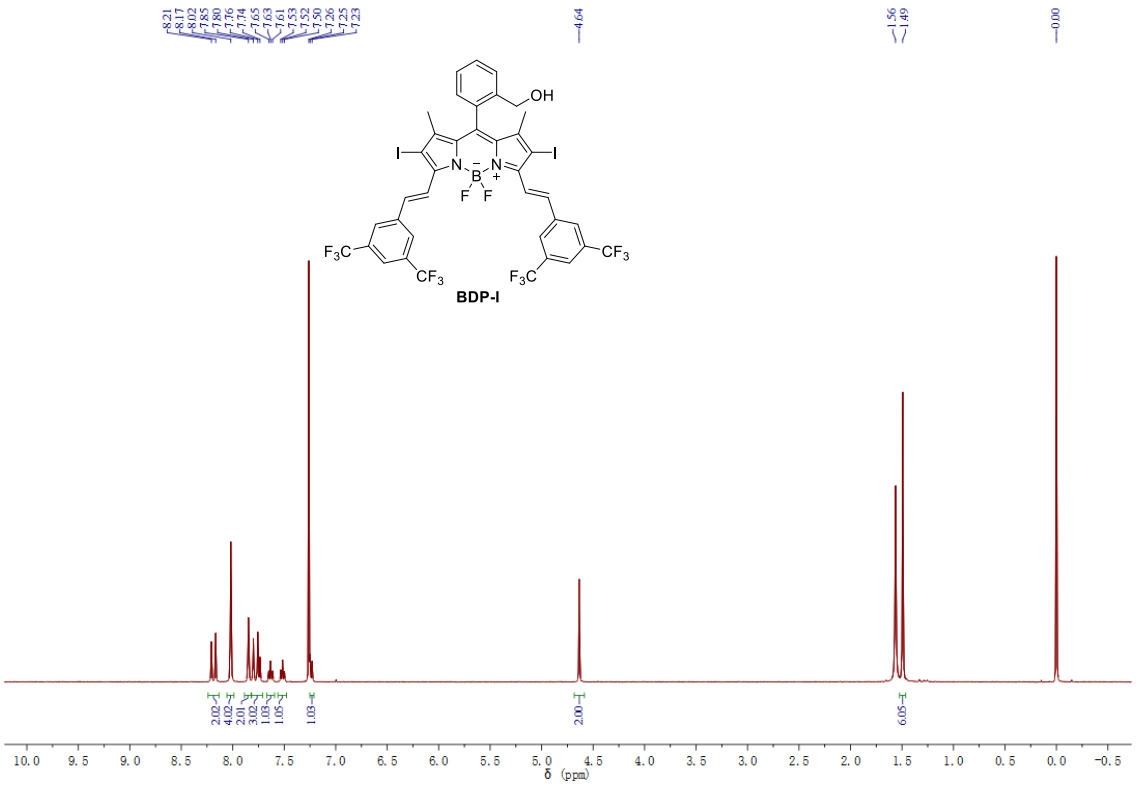

^{1}H NMR of **BDP-I** in $CDCl_3$ (400 MHz).

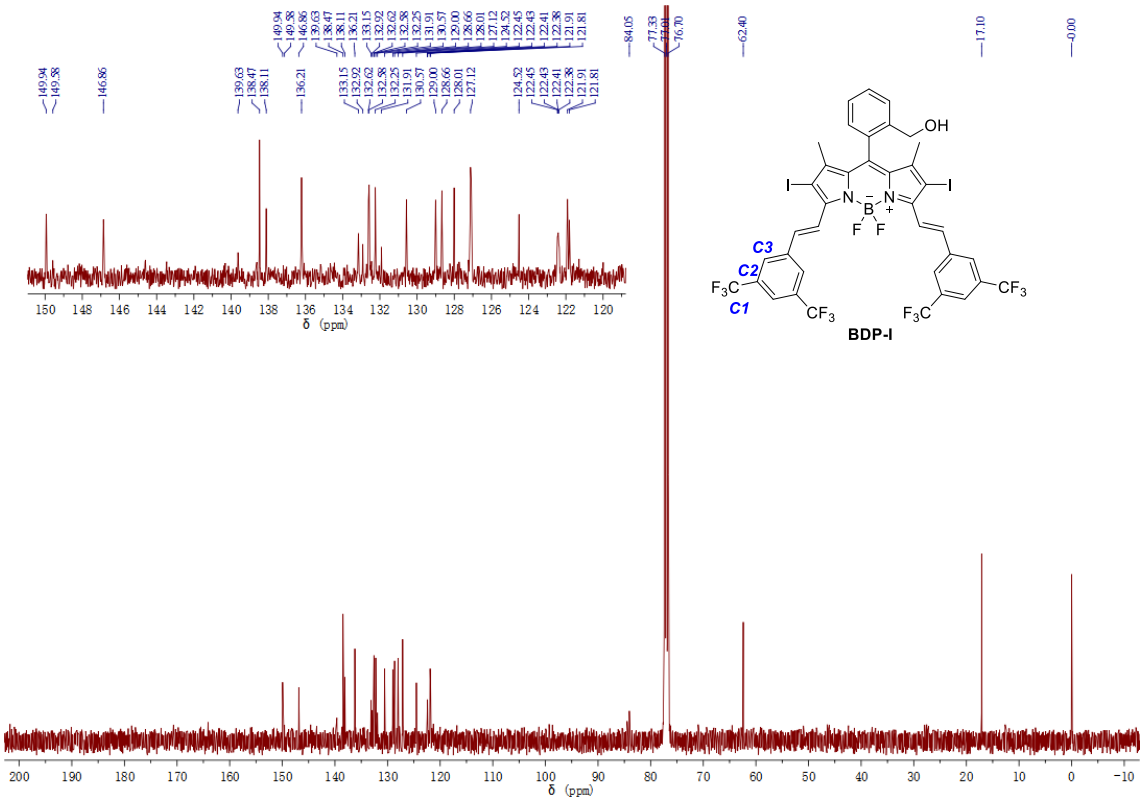

^{13}C NMR of **BDP-I** in $CDCl_3$ (100 MHz).

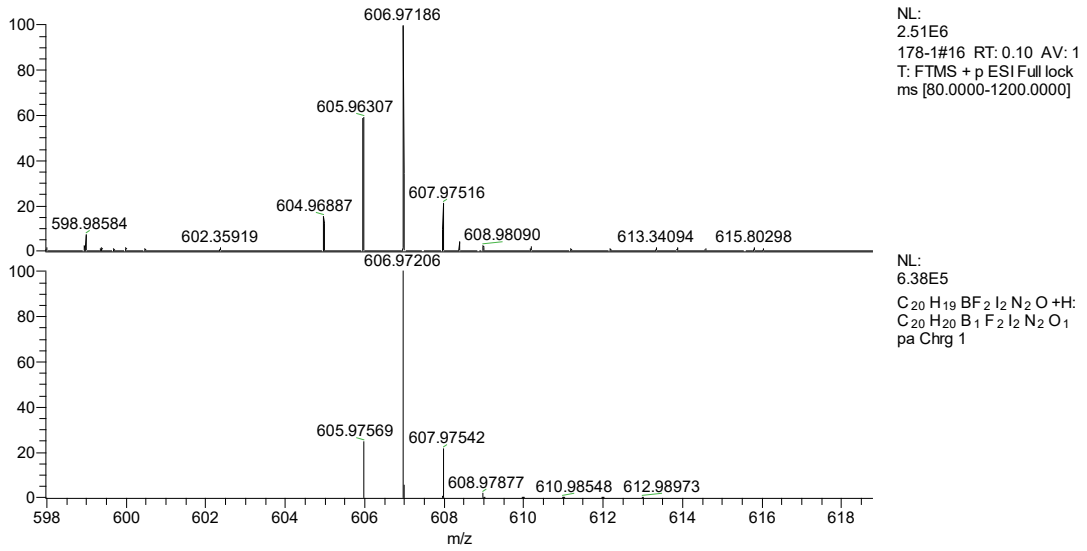

Observed (top) and calculated (bottom) HRMS (ESI) for **2**. For $C_{20}H_{20}BF_2I_2N_2O^+$, $[M+H]^+$: 606.9721, found 606.9719.

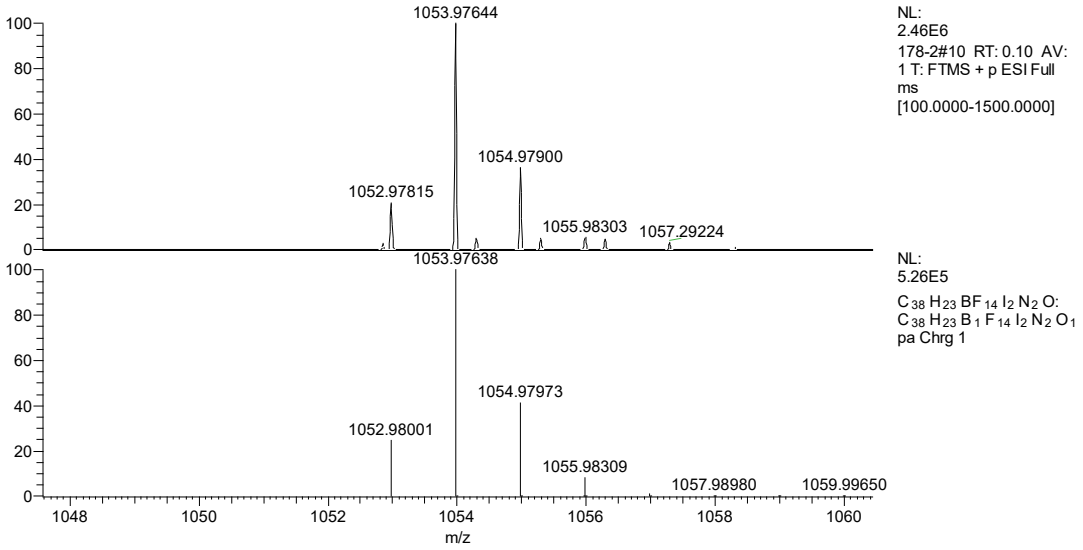

Observed (top) and calculated (bottom) HRMS (ESI) for **BDP-I**. For $C_{38}H_{23}BF_{14}I_2N_2O^+$, $[M]^+$: 1053.9764, found 1053.9764.

7. References

[1] Y. Kawamura, H. Sasabe and C. Adachi, *Jpn. J. Appl. Phys.*, 2004, **43**, 7729.

[2] Gaussian 09, Revision D.01, M. J. Frisch, G. W. Trucks, H. B. Schlegel, G. E. Scuseria, M. A. Robb, J. R. Cheeseman, G. Scalmani, V. Barone, B. Mennucci, G. A. Petersson, H. Nakatsuji, M. Caricato, X. Li, H. P. Hratchian, A. F. Izmaylov, J. Bloino, G. Zheng, J. L. Sonnenberg, M. Hada, M. Ehara, K. Toyota, R. Fukuda, J. Hasegawa, M. Ishida, T. Nakajima, Y. Honda, O. Kitao, H. Nakai, T. Vreven, J. A. Montgomery, Jr., J. E. Peralta, F. Ogliaro, M. Bearpark, J. J. Heyd, E. Brothers, K. N. Kudin, V. N. Staroverov, T. Keith, R. Kobayashi, J. Normand, K. Raghavachari, A. Rendell, J. C. Burant, S. S. Iyengar, J. Tomasi, M. Cossi, N. Rega, J. M. Millam, M. Klene, J. E. Knox, J. B. Cross, V. Bakken, C. Adamo, J. Jaramillo, R. Gomperts, R. E. Stratmann, O. Yazyev, A. J. Austin, R. Cammi, C. Pomelli, J. W. Ochterski, R. L. Martin, K. Morokuma, V. G. Zakrzewski, G. A. Voth, P. Salvador, J. J. Dannenberg, S. Dapprich, A. D. Daniels, O. Farkas, J. B. Foresman, J. V. Ortiz, J. Cioslowski, and D. J. Fox, Gaussian, Inc., Wallingford CT, 2013.

[3] M. H. Lee, N. Park, C. Yi, J. H. Han, J. H. Hong, K. P. Kim, D. H. Kang, J. L. Sessler, C. Kang and J. S. Kim, *J. Am. Chem. Soc.*, 2014, **136**, 14136.

[4] (a) J. N. Schrauben, J. L. Ryerson, J. Michl and J. C. Johnson, *J. Am. Chem. Soc.*, 2014, **136**, 7363; (b) J. C. Johnson, A. J. Nozik and J. Michl, *J. Am. Chem. Soc.*, 2010, **132**, 16302.

[5] X. Zhang, D. Guan, Y. Liu, J. Liu, K. Sun, S. Chen, Y. Zhang, B. Zhao, T. Zhai, Y. Zhang, Q. Li and F. Liu, *Angew. Chem. Int. Ed.*, 2022, **61**, e202211767.

[6] (a) M. H. Lee, J. H. Han, J. H. Lee, N. Park, R. Kumar, C. Kang and J. S. Kim, *Angew. Chem. Int. Ed.*, 2013, **52**, 6206; (b) H. J. Kim, C. H. Heo and H. M. Kim, *J. Am. Chem. Soc.*, 2013, **135**, 17969.

[7] Y. Cakmak, S. Kolemen, S. Duman, Y. Dede, Y. Dolen, B. Kilic, Z. Kostereli, L. T. Yildirim, A. L. Dogan, D. Guc and E. U. Akkaya, *Angew. Chem. Int. Ed.*, 2011, **50**, 11937.

[8] M. del Río, F. Lobo, J. C. López, A. Oliden, J. Bañuelos, I. López-Arbeloa, I. Garcia-Moreno and A. M. Gómez, *J. Org. Chem.*, 2017, **82**, 1240.

[9] Z. Liu, T. Lu and Q. Chen, *Carbon*, 2020, **165**, 461.